An Adaptive Image Watermarking Algorithm Based on HMM in Wavelet Domain[1)]

ZHANG Rong-Yue Ni Jiang-Qun HUANG Ji-Wu

(*Department of Electronic and Communication Engineering, Sun Yat-Sen University, Guangzhou* 510275)

(E-mail: issjqni@zsu.edu.cn)

Abstract An adaptive image watermarking algorithm based on HMM in wavelet domain is proposed. The algorithm is abstracted as follows: 1) the vector HMM model is employed to describe the statistical characteristic of image wavelet coefficients and the resulting HMM based detector achieves significant improvements in performance compared to the conventional correlation detector; 2) adaptive watermark embedding based on HVS analysis; 3) a novel embedding strategy which is optimized for the HMM tree structure is adopted; 4) the strategy of dynamical threshold is applied in watermark detection. High robust results are achieved against Stirmark attacks, such as JPEG compression, adding noise, median cut and filter.

Key words Watermark, hidden markov model (HMM), blind detection, HVS

1 Introduction

With the popularity of internet, the copyright protection of digital media is becoming increasingly important. And thus digital watermarking, especially for image and video, has become the domain of extensive research. Digital watermarking is to embed specific data into original signal. The challenge is that the watermark should be robust against various attacks under the condition of invisibility. Compared with the spacial domain approach, watermarking in transform domain (DCT and wavelet based) can trade off the robustness and visibility, and thus becomes the mainstream in digital watermarking.

From the perspective of digital communication, the wavelet based watermarking can be described as a process of transmission of narrow-band spread spectrum signal over wide-band channel and blind watermark detection is equivalent to the detection of weak signal from strong noise background. Consequently performance of the detector heavily depends on the model of the "channel", *i.e.*, the accuracy of the statistical model for the wavelet coefficients is vital to performance improvement of the detector.

Most of the existing model based wavelet watermarking algorithms are based on the following two assumptions for wavelet coefficients distribution: 1) Gaussian distribution[1] (the correlation detector used in current wavelet based watermarking algorithm implies the gaussian distribution); 2) Generalized gaussian distribution but independent among wavelet coefficients[2,3]. Unfortunately, the first assumption has deviation from the true distribution of wavelet coefficients, while the second one ignores the dependence among wavelet coefficients. In this paper we propose a robust image watermarking algorithm based on the vector hidden Markov model in wavelet domain (WD-VHMM), which takes into account both the energy correlation across the scale and the different sub-band at the same scale of the wavelet pyramid. By incorporating other key technologies such as HVS, optimal embedding structure for HMM tree and dynamical threshold scheme, the proposed WD-VHMM based watermarking algorithm achieves high robustness against Stirmark attacks, such as JPEG compression, median and filtering.

The remainder of this paper is organized as follows. Sections 2 and 3 introduce briefly the hidden Markov model in wavelet domain and the HVS based adaptive watermark embedding scheme, respectively. Section 4 and 5 give the optimal embedding scheme and the blind detection for the vector tree structure. Simulation results and analysis are included in Section 6. Finally, we draw the conclusion in Section 7.

1) Supported by National Natural Science Foundation of P. R. China (60133030, 60172067), Foundation of National Education Ministry of P. R. China

Received November 26, 2003; in revised form June 26, 2005

2 HMM in wavelet domain

Crouse *et al.*[4] points out that, besides its primary properties such as locality, multi-resolution and energy compaction, the wavelet transform has the following two attractive secondary properties:

1) Non-Gaussianity: The wavelet coefficients have peaky, heavy-tailed marginal distributions;

2) Persistency: Large/small values of wavelet coefficients tend to propagate through the scales of the quad-trees.

Taking full advantages of the above properties of wavelet transform, Crouse[4,5] proposed the hidden Markov model in wavelet domain, which can well describe the distribution of wavelet coefficients.

In WD-HMM model, each wavelet coefficient $w_{j,k}(1 \leqslant j \leqslant J,\ j=1$ represents the coarsest scale) has its hidden state $S_{j,k}$. If there is M hidden states, then $P(S_{j,k}=m)=p_{j,k}^{(m)};\ m=1,\cdots,M$. Given $S_{j,k}=m$, $w_{j,k}$ is modeled with a zero-mean Gaussian $g(0,\sigma_{j,k}^{(m)})$. Without loss of generality, we assume $M=2$ in this paper, and the probability density function (PDF) of $w_{j,k}$ is given by the two-state zero-mean Gaussian mixture model as follows.

$$f_j(w)=p_j^1 g(w;\sigma_j^{(1)})+p_j^2 g(w;\sigma_j^{(2)}) \tag{1}$$

where $p_j^{(1)}+p_j^{(2)}=1$, and $g(w;\sigma)=\dfrac{1}{\sqrt{2\pi\sigma^2}}\exp\left(-\dfrac{w^2}{2\sigma^2}\right)$. $p_j^{(1)},p_j^{(2)}$ in (1) represent the probability that $w_{j,k}$ is small or large (in a statistical sense), respectively.

WD-HMM captures the energy dependency across scale by using Markov chain to describe the probability of hidden state transition from the parent node to its four child nodes, *i.e.*,

$$A_j=\begin{pmatrix} p_j^{1\to1} & p_j^{1\to2} \\ p_j^{2\to1} & p_j^{2\to2} \end{pmatrix},\quad j=2,3,\cdots,J \tag{2}$$

where $p_j^{m'\to m}$ represents the probability that child node is in state m given that its parent node is in state m'. The state probability of child node can be determined by that of its parent node and the transition matrix, *i.e.*,

$$p_j^{(m)}=\sum_{m'} p_{j-1}^{(m')} p_j^{m'\to m},\quad j=2,3,\cdots,J \tag{3}$$

If $p_j=(p_j^{(1)}\quad p_j^{(2)})$ and $p_j=p_{j-1}A_j$, then

$$p_j=p_1A_2A_3\cdots A_j,\quad j=2,3,\cdots,J \tag{4}$$

Therefore, the WD-HMM for a tree of wavelet coefficients is completely defined by a set of parameters:

$$\theta=\{p_1,A_2,\cdots,A_J;\sigma_j^{(m)},(j=1,\cdots,J,m=1,2)\} \tag{5}$$

The WD-HMM model can efficiently describe the non-Gaussian behaviors of wavelet coefficients and captures the statistical dependency of wavelet coefficients across scale. Moreover, the efficient EM algorithm exists for fitting a WD-HMM to the observed signal using the ML criterion[4].

The above WD-HMM model is based on the assumption that wavelet coefficients at different orientations are independent, which ignores the existing cross-correlation among sub-band coefficients from different orientations at the same scale. To enhance the capability of WD-HMM in capturing cross-orientation dependency of wavelet coefficient, the vector WD-HMM is adopted in this paper, in which the coefficients at the same location and scale are grouped into a vector (see Fig. 1(b)). Denote the wavelet coefficients at orientation as d ($d=1,2,3$ for H,V,D, respectively), the grouping operation produces vectors of coefficients: $\boldsymbol{w}_{j,k}=(w_{j,k}^{(1)}w_{j,k}^{(2)}w_{j,k}^{(3)})^{\mathrm{T}}$. For vector WD-HMM model, we have

$$f_j(\boldsymbol{w})=p_j^{(1)}g(\boldsymbol{w},\boldsymbol{C}_j^{(1)})+p_j^{(2)}g(\boldsymbol{w},\boldsymbol{C}_j^{(2)}) \tag{6}$$

where $g(\boldsymbol{w};\boldsymbol{C})$ denotes the zero-mean multivariate Gaussian density with covariance matrix $\boldsymbol{C}$, *i.e.*,

$$g(\boldsymbol{w};\boldsymbol{C})=\frac{1}{\sqrt{(2\pi)^n|\det(\boldsymbol{C})|}}\exp(-\boldsymbol{w}^{\mathrm{T}}\boldsymbol{C}^{-1}\boldsymbol{w}) \tag{7}$$

where n is the number of orientations (in this case $n=3$).

The wavelet coefficient vectors in vector WD-HMM have the similar quad-tree structure as that in scalar WD-HMM. Thus an image is modeled by one vector WD-HMM with a set of parameters:

$$\theta = \{p_1, A_2, \cdots, A_J; \boldsymbol{C}_j^{(m)}, (j = 1, \cdots, J, m = 1, 2)\} \tag{8}$$

As the proposed vector WD-HMM model captures both the statistical dependencies of wavelet coefficients across the scale and cross-correlation among subband coefficients at the same scale, it can be expected that the vector model can more accurately describe the statistical behavior of wavelet coefficients.

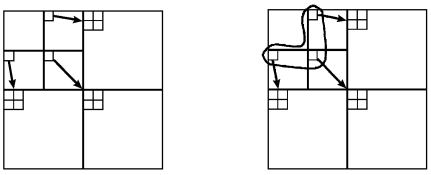

(a) Scalar HMM (b) Vector HMM

Fig. 1 Hidden Markov model in WT (two levels)

3 Human visual system

The human visual system (HVS) plays an important role in digital image processing. It is reported that [6] there are three key masking effects in HVS, *i.e.*, frequency masking, luminance masking and texture masking. The invisible watermarking asks for two contradictory objectives, *i.e.*, robustness and invisibility. Increasing the strength of watermark signal helps to improve the robustness performance, which in turn would decrease the objective of invisibility.

Following Watson′s idea[6], we propose an adaptive watermark embedding strategy incorporating the HVS property. The visual masking weights in wavelet domain are generated based on the HVS analysis for image wavelet coefficients, which are used to control the watermark strength adaptively. Here, three HVS masking features are employed:

1) HVS is less sensitive to noises in middle and high frequency subbands of the wavelet pyramid, so we have the *frequency_m*();

2) HVS has different sensitivity to noise in areas with different background luminance. HVS is almost insensitive to the noise in areas with darker or brighter background luminance, which can be described by the function *luminance_m*();

3) HVS is less sensitive to noise in areas with highly textured patterns, and we have the *texture_m*().

Applying Lewis's result in [7], the perceptual threshold JND is given as follows:

$$JND(j, o, x, y) = frequence\_m(j, o)^* luminance\_m(j, x, y)^* texture\_m(j, x, y)^{0.034} \tag{9}$$

where the definition of the three masking functions in (9) can be found in [6].

4 Watermark embedding

4.1 Watermark embedding based on HMM

Under the framework of vector WD-HMM, the carrier for watermark signal can be depicted by the vector tree shown in Fig. 1(b). In the interest of resisting against JPEG attack, the watermark is embedded only to the coarsest 2 wavelet scales. Therefore each vector tree $\boldsymbol{w}(t)$ which is used to embed watermark includes only 15 nodes, where $w(t, i)$ denotes the i^{th} coefficient of the t^{th} tree.

The process of watermark embedding can be described as follows:

1) The determination of embedding strength $\alpha(t, i)$ based on HVS;

2) The watermark W is chosen to be a PN sequence $s[n]$ of length T, where $s[n] = \{-1, 1\}$;

3) Under the control of secret key k, T vector trees are stochastically chosen within the wavelet domain, where each tree corresponds to 1 bit of the PN sequence. The wavelet coefficients are modified as follows:

$$w'(t, i) = w(t, i) + \beta \cdot s[t] \cdot a(t, i), \quad i = 1, \cdots, 15 \tag{10}$$

where β is the global adjustment factor of embedding strength.

4.2 Optimal embedding

The construction of WD-HMM helps the reliable detection of watermark signal by making use of the difference between the statistical model of image wavelet coefficients (WD-HMM) and that of watermark signal. Therefore the "good" watermark detection strategy is to keep the distance between the models as large as possible under the condition of invisibility.

The embedding rule of (10) makes the child nodes either large or small when one vector tree is modified, and the "distance" between watermark and vector WD-HMM is relatively small. In the interest of reliable detection of watermark, an optimal embedding strategy for the WD-HMM tree structure is developed, which makes half of the child nodes large and others small. Fig. 2(b) shows the optimal embedding structure and (11) gives the optimum embedding rule:

$$\begin{cases} w'(t,i) = w(t,i) + \beta \cdots s[t] \cdot a(t,i), \ i \in 1 \ part \\ w'(t,i) = w(t,i) - \beta \cdot s[t] \cdot a(t,i), \ i \in 2 \ part \end{cases} \tag{11}$$

Simulation results demonstrate that although there is some minor loss in PSNR performance of the watermarked image, the performance against Stirmark attack is significantly improved after the above optimal embedding strategy is applied.

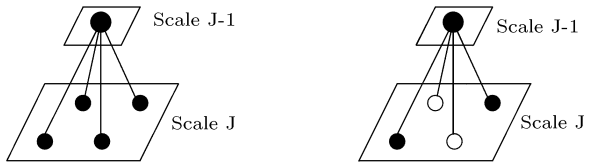

(a) Conventional embedding (b) Optimal embedding

Fig. 2 The strategy for watermark embedding

5 Watermark detection

5.1 Watermark detection based on WD-HMM

Suppose that the image wavelet coefficient $\boldsymbol{x}$ is modeled by a joint probability density function as follows.

$$f_x(\boldsymbol{x}) = \prod_{t=1}^{T} f(\boldsymbol{T}_x^t|\theta) \tag{12}$$

where θ is the set of HMM parameters and $\boldsymbol{T}_x^t$ denotes the t^{th} tree. For an observed image $\boldsymbol{z}$, the watermark detection can be formulated as the following hypothesis test:

$$\boldsymbol{H}_0 : \boldsymbol{z} = \boldsymbol{x} + \boldsymbol{w}^* \text{ and } \boldsymbol{w}^* \neq \boldsymbol{w}; \ \boldsymbol{H}_1 : \boldsymbol{z} = \boldsymbol{x} + \boldsymbol{w} \tag{13}$$

where $\boldsymbol{w}$ is the embedded watermark signal.

5.1.1 The description for the statistics

Given the statistical model $f_x(\boldsymbol{x})$ of original image, the optimal detection can be derived from Neyman-Pearson Theorem [8]:

$$\Lambda(\boldsymbol{z}) = \ln(f_x(\boldsymbol{z} - \boldsymbol{w})/f_x(\boldsymbol{z})) \tag{14}$$

where $\Lambda(\boldsymbol{z})$ is the likelihood function. For given threshold η, we have: $\boldsymbol{H}_1 : \Lambda(\boldsymbol{z}) > \eta$; and $\boldsymbol{H}_0 : \Lambda(\boldsymbol{z}) < \eta$. Incorporating the vector HMM model and vector tree, we have

$$\Lambda(\boldsymbol{z}) = \ln(\boldsymbol{z} - \boldsymbol{w})/f_x(\boldsymbol{z}) = \sum_{t=1}^{T} (\ln f((\boldsymbol{T}_z^t - \beta \cdot s[t] \cdot \alpha_t)|\theta) - \ln f(\boldsymbol{T}_z^t|\theta)) \tag{15}$$

where T represents the length of watermark sequence.

5.1.2 The distribution of $\boldsymbol{\Lambda}(\boldsymbol{z})$ in case of $\boldsymbol{H}_0$

When $\boldsymbol{H}_0$ is true, there is no target watermark signal $\boldsymbol{w}$ in original image $\boldsymbol{x}$. And the observed image $\boldsymbol{z} = \boldsymbol{x} + \boldsymbol{w}^*$, $\boldsymbol{w}^* \neq \boldsymbol{w}$. Denoting $H_0 = \Lambda(\boldsymbol{z})$ in case of $\boldsymbol{H}_0$, we have

$$H_0 = \Lambda(\boldsymbol{z}) = \sum_{t=1}^{T} (\ln f((\boldsymbol{T}_x^t + \beta \cdot s^*[t] \cdot \alpha_t - \beta \cdot s[t] \cdot \alpha_t)|\theta) - \ln f(\boldsymbol{T}_x|\theta)) =$$

$$\sum_{t=1}^{T}(\ln f((\boldsymbol{T}_x^t+\beta\cdot(s^*[t]-s[t])\cdot\alpha_t)|\theta)-\ln f(\boldsymbol{T}_x^t|\theta)) \tag{16}$$

Considering that $s[t]$ and $s^*[t]$ in (16) are PN sequences and take the value 1 or -1 with equal probability, we further obtain

$$p(s^*[t]-s[t])=\begin{cases}0.25, & s^*[t]-s[t]=2\\ 0.5, & s^*[t]-s[t]=0\\ 0.25, & s^*[t]-s[t]=-2\end{cases} \tag{17}$$

Formula (16) can be viewed as the sum of T independent statistics. By applying central limit theorem, we can derive that the PDF of the statistic H_0 is approximately Gaussian with variance σ_0^2 and mean m_0, respectively, where

$$m_0=\sum_{t=1}^{T}\left(\frac{1}{4}\ln f((\boldsymbol{T}_x^t-2\beta\alpha_t)|\theta)+\frac{1}{4}\ln f((\boldsymbol{T}_x^t+2\beta\alpha_t)|\theta)-\frac{1}{2}\ln f(\boldsymbol{T}_x^t|\theta)\right) \tag{18}$$

$$\sigma_0^2=\frac{1}{8}\sum_{t=1}^{T}\{(\ln f((\boldsymbol{T}_x^t+2\beta\alpha_t)|\theta)-(\ln f(\boldsymbol{T}_x^t|\theta)))^2+(\ln f((\boldsymbol{T}_x^t-2\beta\alpha_t)|\theta)-(\ln f(\boldsymbol{T}_x^t|\theta)))^2\}+$$
$$\frac{1}{16}\sum_{t=1}^{T}(\ln f((\boldsymbol{T}_x^t+2\beta\alpha_t)|\theta)-(\ln f((\boldsymbol{T}_x^t-2\beta\alpha_t)|\theta)))^2 \tag{19}$$

5.1.3 The distribution of $\Lambda(\boldsymbol{z})$ in case of $\boldsymbol{H}_1$

When $\boldsymbol{H}_1$ is true, the observed image $\boldsymbol{z}=\boldsymbol{x}+\boldsymbol{w}$, and $\boldsymbol{T}_z^t=\boldsymbol{T}_x^t+\beta\cdot s[t]\cdot\alpha_t$. Also we denote $H_1=\Lambda(\boldsymbol{z})$ in case of $\boldsymbol{H}_1$ and we have

$$H_1=\Lambda(\boldsymbol{z})=\sum_{t=1}^{T}(\ln f(\boldsymbol{T}_x^t|\theta)-\ln f((\boldsymbol{T}_x^t+\beta\cdot s[t]\cdot\alpha_t)|\theta)) \tag{20}$$

Similarly, formula (20) can also be viewed as the sum of T independent statistics. Consequently statistic H_1 is also approximately Gaussian with variance σ_1^2 and mean m_1, respectively, where

$$m_1=\sum_{t=1}^{T}\left(\ln f(\boldsymbol{T}_x^t|\theta)-\frac{1}{2}\ln f((\boldsymbol{T}_x^t-\beta\alpha_t)|\theta)-\frac{1}{2}\ln f((\boldsymbol{T}_x^t+\beta\alpha_t)|\theta)\right) \tag{21}$$

$$\sigma_1^2=\frac{1}{4}\sum_{t=1}^{T}(\ln f((\boldsymbol{T}_x^t-\beta\alpha_t)|\theta)-\ln f((\boldsymbol{T}_x^t+\beta\alpha_t)|\theta))^2 \tag{22}$$

5.2 The correlation detection

The use of correlation detector for watermark signal implies the assumption that the wavelet coefficients are Gaussian. In the interests of fair performance comparison with HMM based detector, we use the similar vector tree structure for watermark embedding. Given the observed image $\boldsymbol{z}$ and hypothesis $\boldsymbol{H}_0$ and $\boldsymbol{H}_1$, the statistic can be formulated as the correlation function

$$\Lambda(\boldsymbol{z})=\rho=\frac{1}{T\cdot I}\sum_{t=1}^{T}\sum_{i=1}^{l}z(t,i)\cdot s[t] \tag{23}$$

where T and I denote the numbers of vector trees and nodes within each tree, respectively. With the similar approach as in section 5.1, we can derive that the PDF of $\Lambda(\boldsymbol{z})$ conditioned to the hypothesis $\boldsymbol{H}_0$ and $\boldsymbol{H}_1$ are approximately Gaussian with variance σ_0^2, σ_1^2 and means m_0 and m_1, respectively, where

$$m_0=0,\quad \sigma_0^2=\frac{1}{T^2\cdot I^2}\sum_{t=1}^{T}\sum_{i=1}^{I}(x^2(t,i)+\beta^2\cdot\alpha^2(t,i)) \tag{24}$$

$$m_1=\frac{1}{T\cdot I}\sum_{t=1}^{T}\sum_{i=1}^{I}\beta\cdot\alpha(t,i),\quad \sigma_1^2=\frac{1}{T^2\cdot I^2}\sum_{t=1}^{T}\sum_{i=1}^{I}x^2(t,i) \tag{25}$$

5.3 The performance criteria for watermark detection

For given threshold η, the probabilities of false alarm and detection are expressed as follows, respectively.

$$P_F = Q\left(\frac{\eta - m_0}{\sigma_0}\right), \quad P_D = Q\left(\frac{\eta - m_1}{\sigma_1}\right) \tag{26}$$

where $Q(\alpha) = \int_{\alpha}^{\infty} \frac{1}{\sqrt{2\pi}} e^{-y^2/2} \mathrm{d}y$.

For design of a good detector, we expect to increase the P_D while keeping the P_F small. Actually, P_D and P_F are two contradictory criteria for any detector. In general, we use ROC, *i.e.*, the receiver operating characteristic, to evaluate the performance of the detector:

$$P_D = Q((\sigma_0 \cdot Q^{-1}(P_F) + m_0 - m_1)/\sigma_1) \tag{27}$$

Given the target false alarm probability P_F, the detection threshold for the resulting HMM detector is[1]:

$$\eta = \sigma_0 \cdot Q^{-1}(P_F) + m_0 \tag{28}$$

6 Simulation results and analysis

In our simulation, we tested a variety of $512 \times 512 \times 8b$ standard images with different texture characteristics, including Lena, Baboon, Fishingboat and Peppers. Fig. 3 shows the original and watermarked image Lena. To demonstrate the effectiveness of the proposed watermarking algorithm, we compare the performance of our HMM based detector versus the conventional correlation detector under StirMark attacks. In the interest of fair performance comparison, the same vector tree structure and watermark signal are used for both detectors.

(a) (b)

Fig. 3 (a) Original image of Lena (b) Watermarked image of Lena

Generally speaking, the increasing strength of attack on watermarked image leads to the smaller H_1. And consequently it increases the probability of miss detection if the threshold η is determined from the un-attacked image. Fig. 4 shows the behavior of H_0 and H_1 when JPEG25 attack is taken on Lena image. It is observed that, although it is impossible to detect the watermark with the original threshold (solid line) η, there still exists enough space between H_0 and H_1 (dot line) to identify the watermark if a dynamical threshold is taken. We also found in our simulation that the statistic H_0 is approximately Gaussian under almost all attacks. Fig. 5 shows the distributions of H_0 under different JPEG attacks. To determine the dynamical threshold for the attacked image, we generate a large sample of PN sequence (say 1000 in our simulation) and compute the value of H_0 for every PN sequence to obtain the m_0 and σ_0^2. For the given $P_F = 10^{-8}$, the dynamical threshold is determined with (28).

The simulation for other attacks under Stirmark 4.1 are taken to test the robustness of the proposed HMM based watermarking algorithm, which include JPEG compression, noise Gaussian filtering, sharpening and median cut. The results are summarized in Table 1∼4.

It can be found from our simulation results that the vector HMM based detector with dynamical threshold has significant improvement in performance with respect to scalar HMM based and correlation detectors. Furthermore, incorporating the optimal embedding strategy leads to further improvement in performance for the vector HMM based detector.

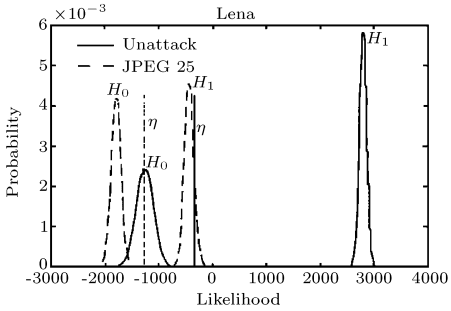

Fig. 4 The behavior of H_0 and H_1 under JPEG25 attack

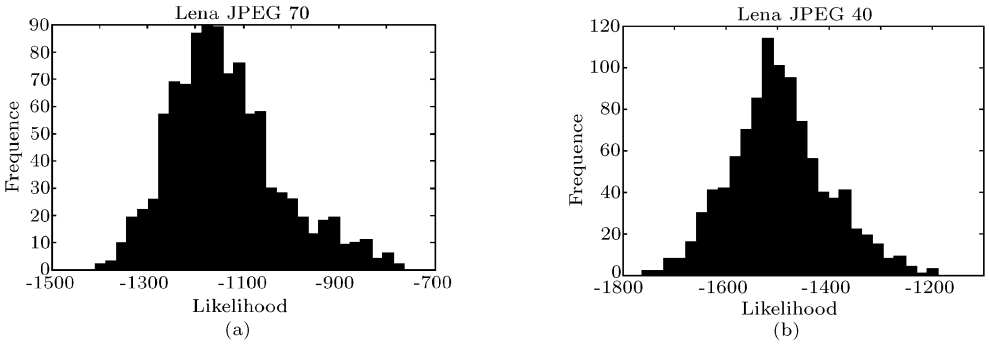

Fig. 5 (a) The distribution of H_0 under JPEG70 for Lena (b) The distribution of H_0 under JPEG40 for Lena

Table 1 Performance of vector HMM detector (conventional embedding)

image	Lena	baboon	f16	Fishingboat	Peppers
PSNR of watermarked image	44.56dB	44.36dB	42.98dB	44.48dB	44.34dB
Best performance of JPEG attack	JPEG19	JPEG7	JPEG15	JPEG13	JPEG14
Best performance of noise attack	9	11	15	12	9
Best performance of median cut	7×7	7×7	7×7	7×7	7×7
Gaussian filter	Ok	Ok	Ok	Ok	Ok
Sharpening	Ok	Ok	Ok	Ok	Ok

Table 2 Performance of vector HMM detector (optimal embedding)

image	Lena	baboon	f16	Fishingboat	Peppers
PSNR of watermarked image	44.59dB	44.36dB	42.95dB	44.49dB	44.33dB
Best performance of JPEG attack	JPEG8	JPEG6	JPEG10	JPEG10	JPEG9
Best performance of noise attack	9	11	12	10	12
Best performance of median cut	11×11	9×9	11×11	11×11	11×11
Gaussian filter	Ok	Ok	Ok	Ok	Ok
Sharpening	Ok	Ok	Ok	Ok	Ok

Table 3 Performance of correlation detector

image	Lena	baboon	f16	Fishingboat	Peppers
PSNR of watermarked image	44.59dB	44.36dB	42.95dB	44.49dB	44.33dB
Best performance of JPEG attack	JPEG42	JPEG28	JPEG23	JPEG40	JPEG43
Best performance of noise attack	6	2	12	5	3
Best performance of median cut	3×3	Fail	5×5	Fail	Fail
Gaussian filter	Ok	Fail	Ok	Ok	Fail
Sharpening	Ok	Ok	Ok	Ok	Ok

Table 4 Performance of scalar HMM detector

image	Lena	baboon	f16	Fishingboat	Peppers
PSNR of watermarked image	44.59dB	44.36dB	42.95dB	44.49dB	44.33dB
Best performance of JPEG attack	JPEG13	JPEG12	JPEG13	JPEG21	JPEG15
Best performance of noise attack	3	2	3	3	2
Best performance of median cut	11×11	5×5	11×11	7×7	9×9
Gaussian filter	Ok	Ok	Ok	Ok	Ok
Sharpening	Ok	Ok	Ok	Ok	Ok

7 Conclusion and the future work

In this paper, we present an adaptive image watermarking algorithm based on the HMM in wavelet domain. The proposed algorithm employs a vector HMM model, which takes into account both the energy correlation across the scale and the different subbands at the same scale of the wavelet pyramid. A novel embedding strategy which is optimized for the HMM tree structure and dynamical threshold scheme are used to further improve the performance. Simulation results show that, compared with conventional correlation detector, our HMM based watermarking algorithm has significant improvement in performance against StirMark attacks, such as JPEG compression, additive noise, median cut and filter.

The objective of the paper is to set up the theoretical framework for HMM based image watermarking and verify its feasibility. Although only the result for 1 bit watermarking is given in the paper, the algorithm can certainly be extended to the cases of multi-bit image and video watermarking, which are the work for further research.

References

1 Hernandez J R. DCT-domain watermarking technique for still image: detector performance analysis and a new structure. *IEEE Transactions on Image Processing*, 2000, **9**(1): 55∼68
2 Cheng Qiang, Huang Thomas S. An additive approach to transform-domain information hiding and optimum detection structure. *IEEE Transactions on Multimedia*, 2001, **3**(9): 273∼284
3 Cheng Q, Huang T S. Blind digital watermarking for images and videos and performance analysis. In: Proceedings of IEEE International Conference on Multimedia and Expos, New York, USA, 2000. **1**: 389∼392
4 Crous M S, Nowak R D, Baraniuk R G. Wavelet-based statistical signal processing using hidden Markov models. *IEEE Transactions on Signal Processing*, 1998, **46**(4): 886∼922
5 Minh N D, Martin Vetterli. Rotation invariant texture characterization and retrieval using steerable wavelet domain hidden Markov models. *IEEE Transactions on Multimedia*, 2002, **4**(4): 517∼527
6 Watson B, Yang G Y. Visibility of wavelet quantization noise. *IEEE Transactions on Image Processing*, 1997, **6**(8): 1164∼1175
7 Lewis A S, Knowles G. Image compression using the 2-D wavelet transform. *IEEE Transactions on Image Processing*, 1992,**1**(2): 244∼250
8 Harry L. Van Trees, Detection, Estimation and Modulation Theory. New York: Wiley, 1968, pt. I.

ZHANG Rong-Yue Received his master degree from Sun Yat-Sen University in 2004. Currently he is a Ph. D. candidate of the same university. His research interests include image/video processing, data hiding, and watermarking.

Ni Jiang-Qun Received his Ph. D. degree from the University of Hong Kong in 1998. Currently he is with the Department of Electronic and Communication Engineering, Sun Yat-Sen University, as an associate professor. His research interests include image/video coding and watermarking, digital communication, and embedded system.

HUANG Ji-Wu Received his bachelor degree from Xidian University, master degree from Tsinghua University and Ph. D. degree from Chinese Academy of Sciences, in 1982, 1987, and 1998, respectively. Currently he is with the Department of Electronic and Communication Engineering, Sun Yat-Sen University, as professor. He is an IEEE senior member and the member of Technique Committee of Multimedia Systems and Applications, IEEE CAS Society. His research interests include image processing, image coding, data hiding, and watermarking.